High Performance Polymer Composites

Subjects: Polymer Science

Contributor: Dmitry Buslovich

Summarize data on the structure, mechanical and tribological properties, and wear patterns of composites based on high-performance polymers (HPPs) intended for use in friction units. The three key sections, divided according to the tribological contact schemes regardless of the polymer matrix. In the second part, the analysis of composites is carried out in point contacts. The third section is devoted to the results of studies of HPP-based composites in linear ones. The fourth section summarizes information on flat contacts. Particular attention is paid to the formation of transfer films (TFs) in the contacts and their influence on the tribological patterns of the studied rubbing materials.

high-performance polymers | antifriction composites | transfer film | wear rate

1. Introduction

A number of such materials are described in excessive detail in the literature, in particular, neat polyetheretherketone (PEEK) and PEEK-based composites, while a similar polyaryletherketone (PAEK) polymer has rarely been the subject of research. At the same time, polytetrafluoroethylene (PTFE) is not included in this list as a matrix material, despite the fact that it is extremely widely used as solid lubricant filler. The authors are aware that such an effect is associated primarily with the difference in conditions of tribological tests, including a loading scheme (a contact type), load-speed (P·V) parameters, temperatures and environments, and the counterpart material and its roughness, etc. For this reason, the conditions of the tribological tests are characterized in the description and analysis of the obtained results.

As a key criterion (the top level of the classification), a contact scheme of the polymer composites and counterparts (namely, point, line, and flat ones) is adopted since it determines the macroscale level of the tribological interaction of the rubbing bodies. The influence of other parameters is considered when interpreting reported values of the coefficient of friction (CoF) and wear rate (WR), as well as the characteristic mechanisms that determine an increase/decrease in wear resistance.

The prospect of using HPPs to design materials for friction units is determined by their two key properties: high melting points and great strength properties. In addition to an acceptable level of melt flow index and the ability to provide interfacial adhesion to filler particles/fibers (including at a sufficiently high degree of their content), these materials are also attractive because of their ability to process and improve the stiffness/load-bearing capacity. However, advanced strength properties of this class of materials simultaneously determine great CoF levels, which in most cases can exceed 0.3 on steel under dry sliding friction (DSF) conditions. According to Brian J. Briscoe, a

typical method for solving this problem is loading polymers with various types of fillers using the ‘hard and strong fillers in a softer matrix’ or ‘soft and lubricating fillers in a hard and strong matrix’ principles [1].

Recently, special attention has been paid to loading metals and nonmetal oxides (in particular, SiO_2, SiC, ZnO, TiO_2, Al_2O_3, Si_3N_4, CuO) with nanoparticles as a way to improve the load-bearing capacity and wear resistance of the polymer composites against counterparts [2]. In addition, a large number of researchers studying the composites have loaded carbon nanotubes (CNTs) with the goal of enforcing polymers since CNTs show very high strength and stiffness.

Regardless of the types of loaded fillers, the invariable condition for enhancing wear resistance is the formation of a thin and uniform transfer film (TF) or transfer film layer (TFL) and its reliable adherence on a counterpart. Thinner TFs tend to adhere stronger to counterpart surfaces than thicker ones. In this regard, the emphasis in interpreting the results of tribological tests of polymer composites is shifting toward the specifics of the TF formation and fixation on the counterparts. Additionally, there are two conditions that determine the ability of a polymer composite to form such a film: (1) loss of the polymer material by attrition due to interaction with metal asperities; and (2) its ability to be adhered and retained on the counterpart surface for a long time. The latter process is hindered by the loss of the TFs via debonding from the counterparts [2]. A third important effect on the wear process should also be added, namely, the formation of oxidized debris in the tribological contact zones, including from the fractured TFs. They can both exert an abrasive effect and act as a third body that facilitates sliding.

As an effective approach for designing antifriction polymer composites, Li Chang [3] analyzed the formation of hybrid materials that simultaneously include both solid lubricant particles and reinforcing fibers. The synergetic principle of their action characterizes a scheme in **Figure 1**. The following are noted as key tribological aspects [3]: (1) The pin-on-disc (P-o-D) and block-on-ring (B-o-R) schemes are two generally used methods for sliding wear tests. (2) The presence of reinforcing fibers strengthens the polymer composites and protects them against irregularities (asperities) on the counterpart surfaces on the one hand. On the other hand, hard fibers can damage the counterpart surfaces and prevent TFs from attaching to them. Finally, the author concluded that ‘understanding of the growth of TFLs and their tribological behavior during steady state wearing stage is still limited owing to the lack of quantitative techniques’ [3]. Note that researchers of HPP-based composites put very different concepts into the TF term despite the obviousness of the wear process development. For this reason, the TF role in the formation of the tribological properties can be both negative and positive, even providing friction in the ‘wearless’ mode.

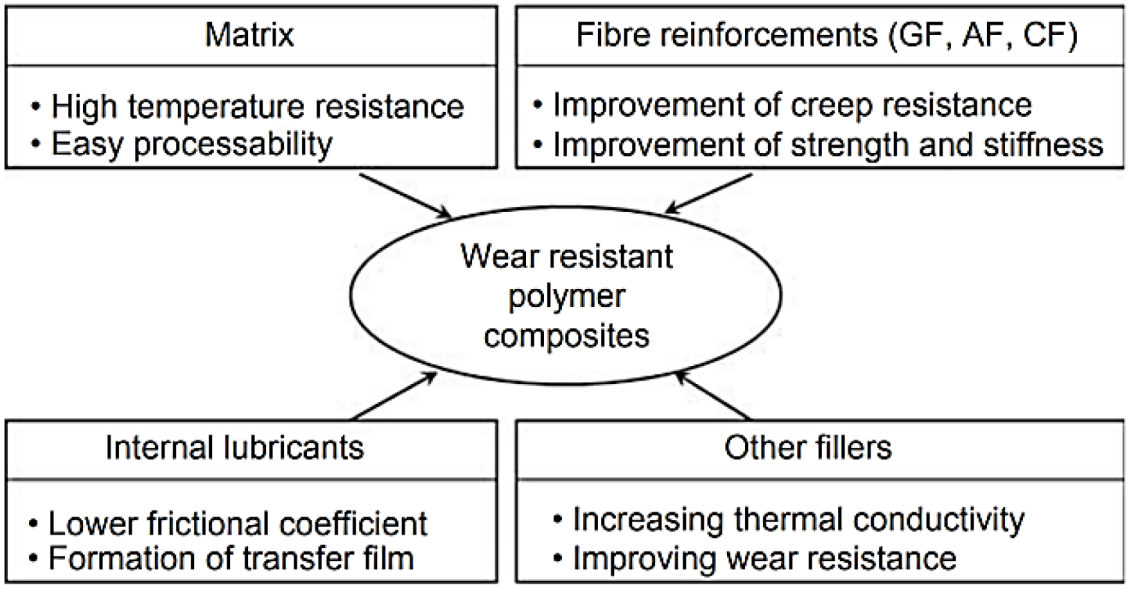

Figure 1. A summary of the structural components of the wear resistant polymer composites. Figure is reproduced with permission from reference [3].

In [4] Meghashree Padhan suggested some examples of hybrid 'PEEK + PAEK'-based composites loaded with 30% short carbon fibers (SCFs) and 10% graphite (Gr) nanoparticles as primary solid lubricants (SLs), as well as 10% noncarbon secondary SLs such as WS_2, MoS_2, h-BN, etc. When interpreting the results, the effect of synergism between both types of SLs and the best efficiency of nanoparticles over microsized inclusions were considered.

The widespread use of nanofillers to improve wear resistance of polymer composites has prompted a significant number of reviews. For example, Qihua Wang emphasized [5] that nanoparticles alter friction and wear behavior in different ways. As a result, low CoF levels do not necessarily correspond to decreased WR values. At the same time, the factors affecting wear resistance are types of the combined polymer and nanoparticles, the filler content, and the friction contact size and shape in addition to operating conditions. Due to so many influencing factors, the effect of nanoparticles on the tribological properties of the antifriction polymer composites is still an open field for further research. This is especially the case when nanoparticles in combination with conventional fillers are considered. In doing so, a detailed analysis of the tribological behavior of various types of the composites with explicit consideration of the specific conditions of tribological tests is required.

A modification of M. Ashby's concept on ranking structural materials over multidirectional functional properties [6] has been suggested for designing polymer composites for tribological purposes [7]. It considers WR, CoF and tensile strength levels of the polymer matrix, etc. (**Figure 2**). This approach is important due to its versatility since it enables the solution of the practically important issues of choosing polymer composites (including multicomponent ones) for given operating conditions. However, as noted above, the tribological properties depend on a number of parameters, so it is almost impossible to offer a completely universal approach within the framework of such data. As a result, a promising research area is the implementation of machine learning algorithms [3].

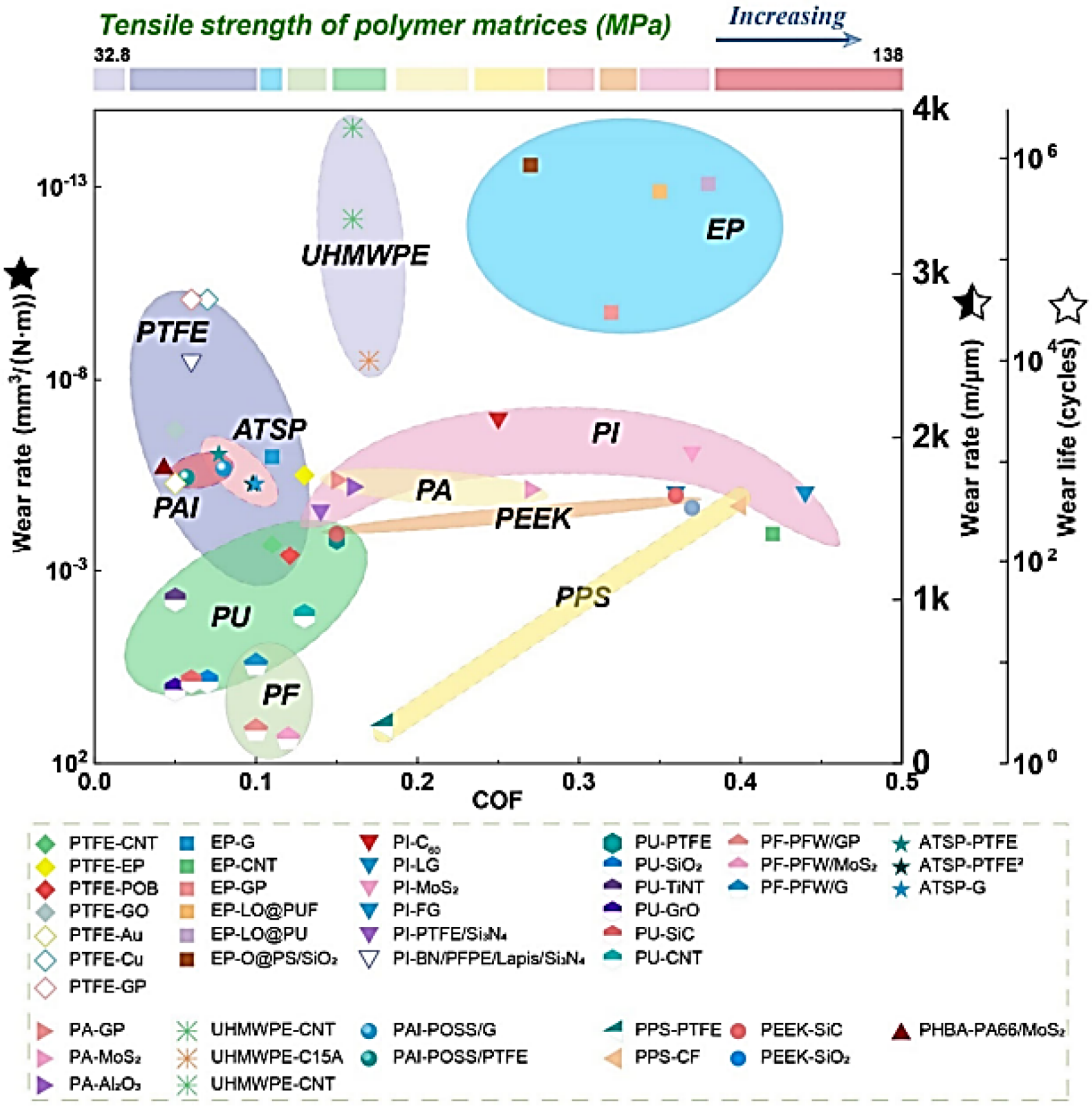

Figure 2. The tribological properties of different polymer matrices and fillers. Figure is reproduced with permission from reference [7].

The demand for HPPs in various industries has prompted a variety of reviews on their functional properties. In particular, Kurdi, A. et al. discussed the wear mechanisms under sliding friction for designing high-performance composites [8]. In this case, special attention was also paid to environmental factors, namely lubrication conditions, temperature, and even the possibility of developing vibration-induced phenomena. It was noted that loading with fillers may cause discontinuities in the polymer matrix, which promote the formation of debris. As a result, the critical filler contents should be limited to 5–15 vol.%. The role of nanoparticles in changing wear resistance narrows to both probable rolling effect and topographic smoothening of the friction surfaces. Similar to other authors in this field of science, Kurdi, A. and Chang, L. noted that the desired effect is achieved mainly by using a combination of reinforcing particles and fibers. However, an increase in both strength and toughness of HPPs does not always reduce the intensity of the wear mechanism development and the formation of debris.

Neat HPPs are not antifriction materials due to their high strength, which inhibits easy sliding on the counterpart (primarily steel) surfaces., This challenge is overcome in the design of composites by loading solid lubricant particles, followed by TF formation on the counterparts. However, the number of asperities on the sliding surfaces, determining CoF levels, also depends on the contact area. Three contact types are typically distinguished in tribology: point, line, and area (**Figure 3**) [4]. It is not too difficult to form a TF that is uniform in thickness and relatively firmly adhered on the surface of a steel ball at a point contact; however, this task becomes highly complicated for area contact types. The reason is lower specific pressures for this tribological loading scheme (as a rule). Temperature is another important aspect, since it is easier to realize heating followed by tribological oxidation and adhesion in a point contact than in both line and area ones.

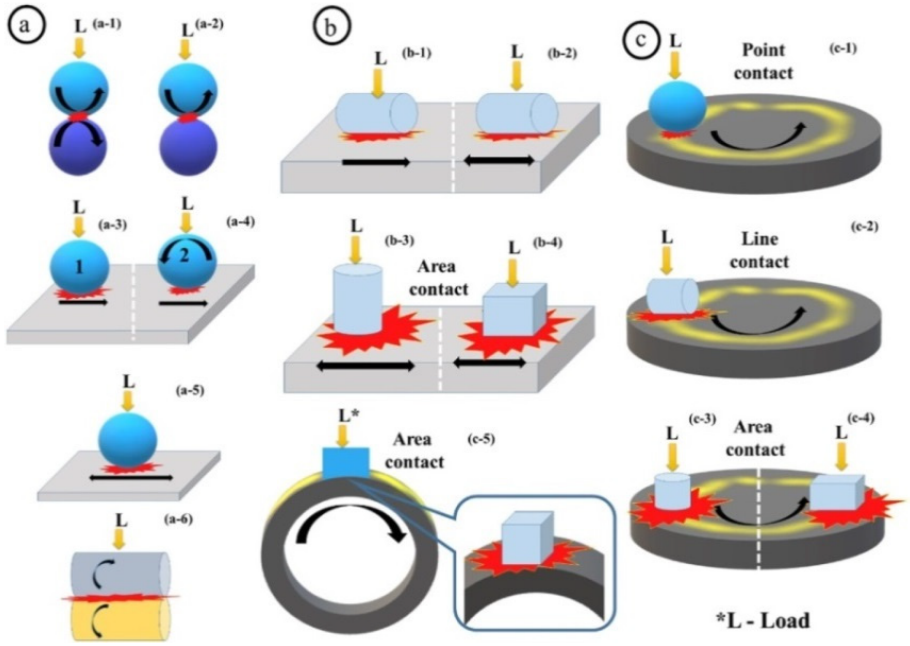

Figure 3. Various tribo-configurations and tribo-contacts: point contact (**a-1** to **a-5** and **c-1**), line contacts (**a-6**, **b-1** and **c-2**) and area contacts (**b-2**, **c-3** and **c-4**). Rotary motion (**a-1**, **a-2**, **a-4**, **a-6**, **c-1**, **c-2**, **c-3**, **c-4** and **c-5**), Reciprocating linear motion (**a-5**, **b-2**, **b-3**, **b-4**), linear forward motion (**a-3**, **a-4** and **b-1**). Figure is reproduced with permission from reference [4].

HPPs include polyethersulfone (PES), polyetherimide (PEI), polyphenylene sulfide (PPS), PEEK, fluoropolymers, etc. Their attractiveness lies in the possibility of replacing metal parts with nonmetallic ones in high-tech industries [9]. However, most papers on HPPs for tribological applications focus on a limited number of thermoplastics such as PPS, PEEK, and polyimide (PI). In this regard, numerous loaded fillers, their combinations, as well as schemes and conditions of tribological tests should be investigated on this topic.

A significant number of papers on the use of PEEK-based composites are devoted to orthopedic applications. The authors are looking for ways to replace metal implants (components) with polymer ones, for which neat PEEK is often loaded with CFs [10]. In the design of PEEK-based composites for biomedical engineering applications, aspects of the polymer-filler interfacial interaction and their fabrication methods also play an important role.

Oladapo et al. [11] noted perspectives of the PEEK-based composites from the point of view of the implementation of additive manufacturing (AM) procedures. Also, cellular calcium hydroxyapatite (CHAp) was analyzed as an advanced excipient. Another review [12] is devoted to the use of PEEK for designing biomedical composites and highlights its relevance in dental applications as well. In addition, PEEK is widely used for manufacturing knee, hip, spine and other implants in orthopedics. A review on dental applications of PEEK is given in [13]. Further analysis of the issue in its application for scaffolds was carried out by the authors of [14]. In a similar paper [15] Ma, H. et al. summarized some aspects of the performance requirements, the composite design process, and the surface modification when using PEEK as a material for the manufacture of orthopedic implants.

Because the tribological properties of the polymer composites are determined by their friction surfaces, some data on the PEEK surface modification have also been reviewed. In [16], Singh, S. analyzed plasma treatment of PEEK in terms of its influence on the biological, surface (adhesion and wettability), mechanical, and tribological properties. As noted above, some similar materials are gaining popularity in the development of HPP-based composites. In their review [17] Veazey, D., et al. proposed a roadmap for high-performance PAEK-based composites reinforced with long fibers (**Figure 4**). They emphasized that one of the key challenges in designing these composites is improving the fiber-matrix interfacial bond strength.

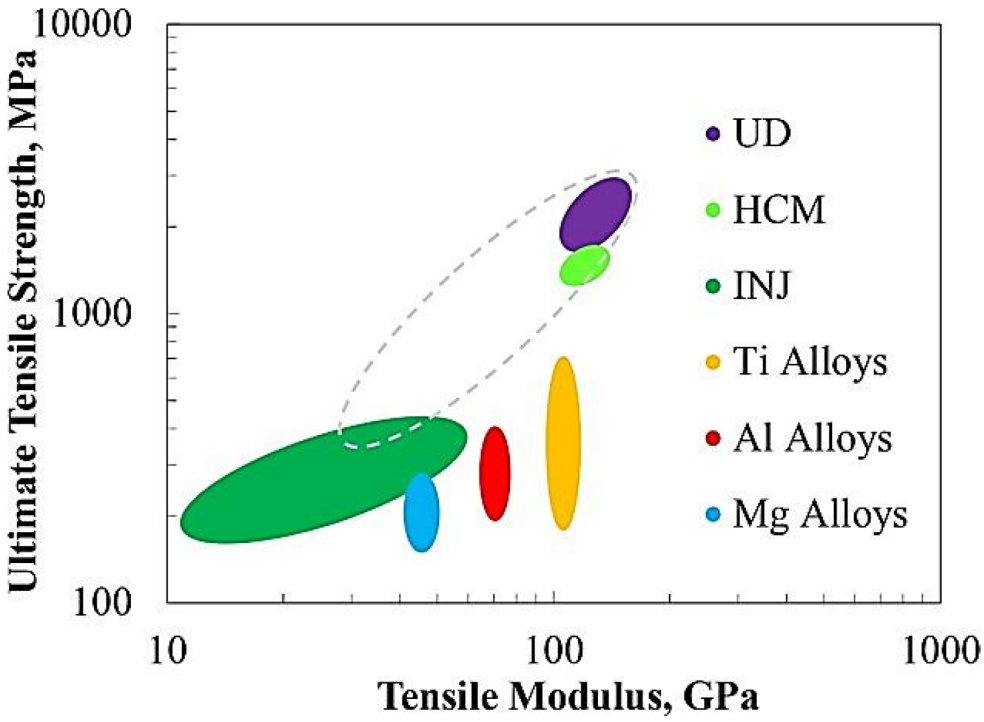

Figure 4. Typical tensile properties of common metallic alloys and CF-reinforced PAEK-based composites: UD, unidirectional fibers; HCM, hot compression molded fibers; INJ, injection molded fibers. Figure is reproduced with permission from reference [17].

The unique properties of PI have determined the prospects for some practical applications of PI-based composites. The most detailed review [18] covers the issues of their synthesis. It has been shown that the presence of functional

groups and the formation of dendritic structures enable unique properties in PI-based composites. Their key advantage is the possibility of high-temperature applications. Nevertheless, some design challenges remain for the PI-based nanocomposites. For example, Ogbonna, V.E. emphasized [19] some issues of interfacial adhesion and surface degradation, which affect their mechanical properties and abrasive wear resistance in tribological applications. The following are considered fillers for such PI-based nanocomposites: CNTs, GN, graphene oxide (GO), boron nitride (BN), MoS_2, silica (SiO_2), titania (TiO_2), alumina (Al_2O_3), CFs, aramid fibers (AFs), GF, zinc dioxide (ZnO_2), zirconium dioxide (ZrO_2), silicon nitride (Si_2N_4), and carbon nitride (C_3N_4). In [20] nanofillers of the mentioned types were reviewed from the standpoint of their influence on the structure and mechanical properties of the PI-based nanocomposites. Also, similar to the PEEK-based composites, the PI-based ones are used in medical applications. Some chemical, physical, and manufacturing aspects of designing the PI-based biocompatible composites are summarized by Catalin P. Constantin in [21].

2. Point Contacts

2.1. Neat HPP

In [22] Puhan, D. et al. tested neat PEEK on both steel and sapphire counterparts. It showed that the chemical compositions of the formed TFs differ from that of neat PEEK. The TFs mainly consisted of amorphous carbonaceous materials. Molecular chains of PEEK were broken in different positions of the ester and ketone groups. Additionally, opening of aromatic rings, substitution, and cross-linking, as well as both crystallinity and coplanarity losses were reported. As shown in **Figure 5**, a carboxylic acid formed, the interaction of which caused the formation of thin and strong TFs during friction with the surfaces of the steel or sapphire counterpart *(PEEK; R_a = 1–1.2 µm; B-o-D; counterpart is a ball with a diameter of 6 mm; R_a = 0.02 µm; P = 10 N; V = 2 m/s; L = 3.6 km; P_{max} = 160 MPa).*

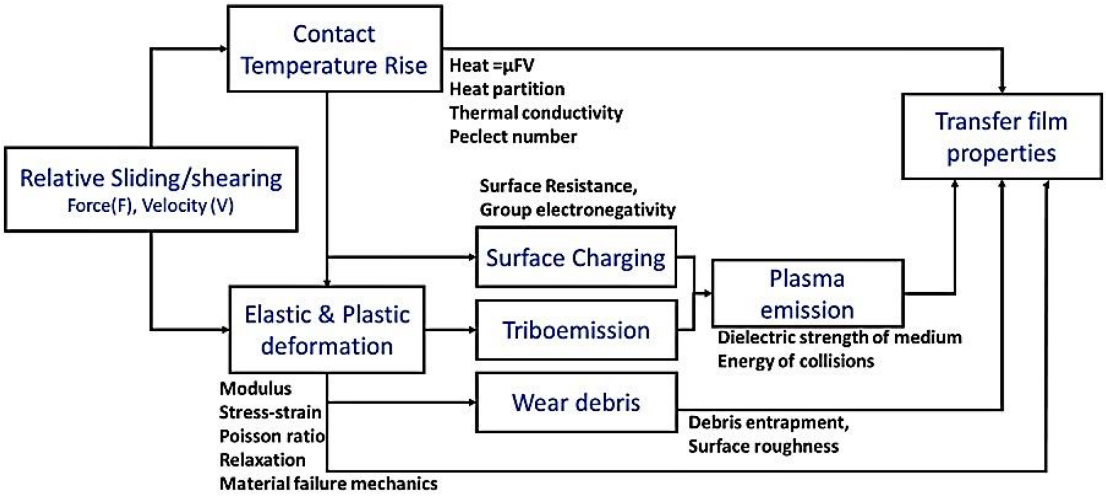

Figure 5. Factors effecting functional properties of polymeric TFs upon sliding PEEK on the steel surfaces. Figure is reproduced with permission from reference [22].

A number of papers are devoted to the effect of various surface treatment procedures on the tribological properties of PEEK. For example, Wang, M. showed the influence of engineered surface microstructuring on friction patterns in PEEK-steel contacts [23]. Pronounced fluctuations of CoF curves were observed in both nontextured and textured PEEK containing microholes with a diameter of 25 μm. This was accompanied by the formation of a noticeable amount of debris. In the case of friction of the GCr15 steel ball on the microtextured PEEK surface with holes 50 μm in diameter, the WR level was reduced sharply *(PEEK; GCr15 ball; RF; R_a = 0.02 μm; B-o-F; DSF; LF = 0.9 and 3 N).*

Cho, M. investigated the ability of PPS to form a TF while sliding on steel [24]. The steel counterpart surfaces were textured with four pore densities of 5, 15, 25, and 35% using a laser. Then, pores were filled with PPS powder followed by curing. This hybrid texturing protected the steel surfaces with formed TFs. An effective decrease in CoF levels was observed for the surface with the pore density of 5% at V = 0.15 m/s, in contrast to both V values of 0.05 and 0.10 m/s since high sliding speeds favored TF formation. In the case of the pore density of 15%, the CoF values were decreased for all sliding speeds, because TFs of moderate thicknesses covered all wear tracks *(PPS; B-o-D; 100Cr6 steel ball; R_a = n/d; DSF; V = 0.05, 0.10, and 0.15 m/s; P = 9.8 N; L = 360 m)*.

Duan, C., et al. analyzed aspects of the influence of the PI molecular structure on the mechanical and tribological properties under conditions of incorporation of 4,4′-ODA into polyimide with 3,4′-ODA isomer [25]. It was shown that CoF levels were lowered with raising the 4,4′-oxydianiline (4,4′-ODA) content in the PI macromolecular chains. These changes were related to the macromolecular chain conformation caused by different monomer configurations. Thus, PI with paraposition diamine exhibited the best tribological properties *(PI; B-o-F; RF; counterpart is the GCr15 steel ball with a diameter of 3 mm; R_a = n/d; P = 5 N; V = 0.1 m/s; Ampl = 2.5 mm; T = 20 °C; RH = 16–20%; L = 300 m).*

In [26] Fareed, M. I. studied the tribological properties of PEEK by varying its structure through various heat treatment procedures such as annealing, normalizing, and both water and oil quenching from a temperature of 250 °C. The PEEK crystallinity reduced with an increase in its cooling rate. At the same time, the lowest crystallinity was found after water quenching. Conversely, the annealed samples showed the highest wear resistance because of the enhanced crystallinity. For each of these heat treatment procedures, WR levels increased with rising normal load *(PEEK; B-o-D; Stainless steel ball; R_a = n/d; P = 30, 60, 90 N; V = 62.8 mm/s; L = 62.8 m; DSF).*

Lubricating medium in a tribological contact changes conditions of TF formation. Tatsumi, G., et al. evaluated the role of organic friction modifiers (OFMs) in the lubrication improvement in PEEK-steel contacts [27]. Compared with OFM-A (oleylamine) and OFM-B (oleic acid), OFM-C (N-oleoyl sarcosine) showed a significant reduction in CoF levels in the ‘PEEK-smooth steel’ friction pair by 200% under sliding conditions and by 50% under the sliding-rolling ones. A similar CoF reduction was observed for OFM-C in both ‘PEEK-PEEK’ and ‘steel-steel’ friction pairs. A clear correlation between thicknesses of the PEEK TFs and the tribological properties of the ‘PEEK-steel’ friction pair was found. OFM-C exerted a great impact on these characteristics due to its ability to be strongly absorbed on both materials (**Figure 6**), inhibiting PEEK TF formation. This had both positive and negative effects on the tribological

properties depending on the test conditions *(PEEK; B-o-P; sliding/sliding-rolling; R_a = n/d; V = 1 m/s; P = 50 N (PEEK-steel and PEEK-PEEK); P = 5 N (steel-steel); T = 25 °C).*

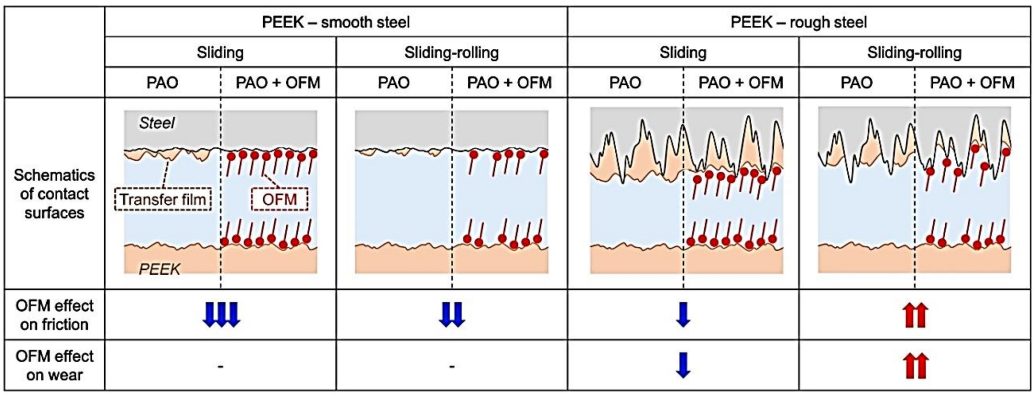

Figure 6. The OFM lubrication mechanism in the PEEK-steel contacts. Figure is reproduced with permission from reference [27].

An important aspect that determines the development of the tribological processes is temperature in the friction contacts. Laux, K.A., et al. used infrared thermography to observe the full field temperature map of PEEK upon its sliding on both stainless steel and sapphire counterparts [28]. It was shown that PEEK debris attaches easily to the steel counterpart but not to the sapphire one. The PEEK transfer to the steel surface may be accompanied by an increase in the sliding interface temperature (up to T_g). The PEEK TF was essentially oriented towards the steel counterpart surface. For this reason, TF formation was determined by the friction processes and the tribological contact temperature, which are not functionally dependent on the load-speed parameters *(PEEK; B-o-D; counterparts are the sapphire ball with a diameter of 19 mm (R_a = 1.5 µm) and the 52,100 steel disc 46 mm in diameter (R_a = 10 nm); T = 25 °C; P = 1–40 N; V = 100 mm/s).*

Yahiaoui, M., et al. studied the tribological behavior of the PEEK-steel contact in reciprocating or unidirectional motion by varying load, speed, and sliding distance [29]. CoF values were reduced due to lowering the load that decreased the contribution of molecular attraction forces, as well as because of the rising speed that cumulated the mechanical energy. The reason was the adiabatic effect in the contact, which changed the polymer rheology. As a result, two interfacial mechanisms were identified (**Figure 7**). The first one was the formation of Schallamarch ridges due to nanoscopic interaction between them. The longitudinal ploughing mechanism was responsible for the formation of microscopic scratches. During reciprocal sliding, the polymer relaxation strongly affected its tribological behavior. Unidirectional sliding caused greater plastic strains and stretched Schallamarch ridges in the sliding direction *(PEEK; B-o-F; counterpart is the 100Cr6 steel ball with a diameter of 6 mm; reciprocating or unidirectional motion: (i) V = 100 mm/min, L = 250 mm, P = 1–30 N; (ii) P = 30 N, L = 250 mm, V = 10–500 mm/min; (iii) Ampl = 5 mm, L = 0.005–3.710 m; PEEK; R_a = 65 ± 9 nm).*

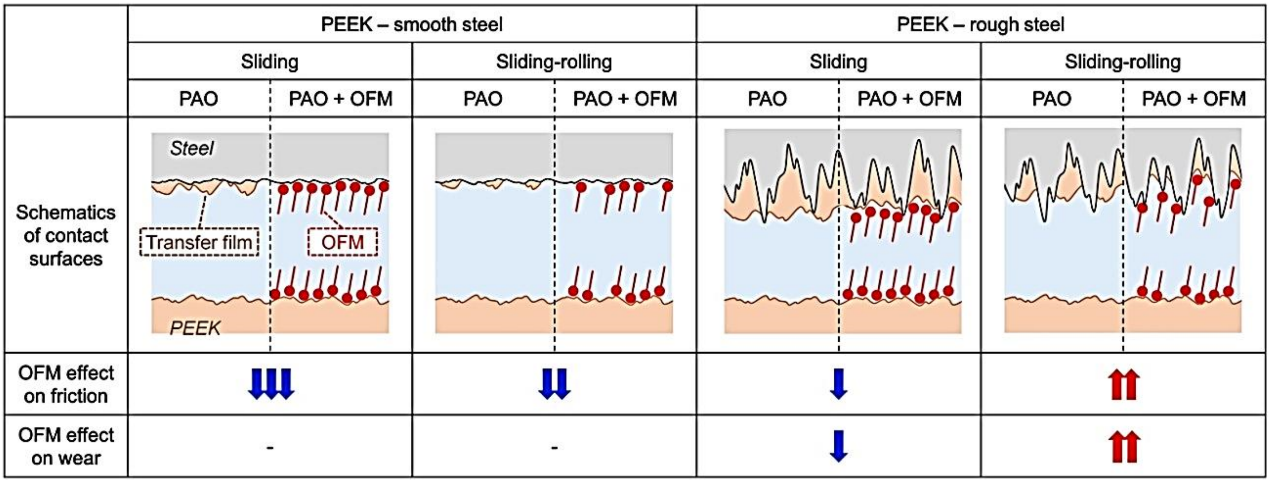

Figure 7. The cohesive and interfacial contact mechanisms as a function of the cumulated mechanical energy. Figure is reproduced with permission from reference [29].

For HPPs, one of the limiting factors for wear resistance is the (T_g) glass transition temperature. Jean-Fulcrand, et al. solved this issue by combining polybenzimidazole (PBI), having one of the highest T_g points, with PEEK in a ratio of 50:50 [30]. Chemical analysis of TFs formed on the steel counterpart surface and debris in the tribological contact showed the polymer degradation caused by shear heating. In the case of the 'PEEK + PBI' composite, TFs formed on the steel counterpart and possessed a composition similar to that of PEEK. When the contact temperature was close to the PEEK melting point, PEEK, as a composite component, formed a thin TF that acted as an interfacial lubricant. This reduced CoF levels, which in turn decreased the PBI degradation in the composite at high temperatures *(PEEK-PBI; B-o-D; T = 100, 190, and 280 °C; DSF; V = 0.1–2.0 m/s; L = 3.6 km; P = 10 N; HAP = 116, 124 and 138 MPa; R_a(PBI) = 1.41 ± 0.43 µm; R_a(PEEK-PBI) = 1.27 ± 0.18 µm; R_a(PEEK) = 0.79 ± 0.15 µm; R_a(Steel) < 0.01 µm).*

In [31] Zhang, G., et al. analyzed the effect of the amorphous structure of a PEEK film on its tribological properties. It was shown that there is no relative movement between a ball and the amorphous PEEK surface during the stick-slip sliding process due to the adhesion force in the interface zone. As a result, the material accumulated ahead of the counterpart. During the stick stage, shear stresses were less than the critical level required for adhesion between the sliding parts, but it increased with time. At high levels of the applied load, the tribological properties of amorphous PEEK could be closely related to its viscoelastic behavior, while the dominant factor was the 'ironing' effect at low load-speed levels. The change in the tribological properties of amorphous PEEK with an increase in sliding speed may be associated with the rising interfacial temperature. The critical load may be lower than that at which there is no pronounced viscous flow *(PEEK; B-o-D; T = 20 °C; RH = 70%; counterpart is the 100Cr6 steel ball with a diameter of 6 mm; R_a = 0.02 µm; L = 2 km; P = 1–9 N; V = 0.2–1.4 m/s).*

2.2. Reinforced HPP-Based Composites

Yamaguchi, T., et al. investigated wearing of PEEK-based composites loaded with particles of rice bran ceramics (RBC) under water lubrication (WL) conditions [32]. The 'PEEK + RBC (10–40 wt.%)' samples showed a decrease

in both CoF and specific WR values over a wide range of the P·V conditions compared to those for neat PEEK. The authors suggested that the reason was the hydrodynamic lubrication effect. *(PEEK; B-o-D; R_a = 0.14 µm; counterpart is the SUS 304 steel ball with a diameter of 8 mm; WL; V = 0.1–2.0 m/s; P = 0.98–9.80 N)* Dong, F., et al. assessed the friction and wear behavior of neat PI and 'PI + CF' reinforced composites at various temperatures [33]. Loading with CFs significantly improved wear resistance over the entire temperature range, and CoF levels were highly dependent on the sliding contact temperature. It was found that the CF lubricity appeared only at high temperatures of 180–260 °C, which could be explained by their graphitization and subsequent TF formation on the worn surfaces with excellent lubricity *(PI; B-o-D; R_a = 0.03 µm; counterpart is the GCr15 steel ball with a diameter of 3 mm; R_a = 0.02 µm; V = 0.3 m/s (573 r/min); P = 5 N; t = 30 min).*

Lv, M., et al. reported the tribological behavior of PI-based composites reinforced with CFs and AFs under simulated space irradiation conditions and during the 'start-stop' friction process [34]. Loading with CFs and AFs contributed to lower CoF values and improved wear resistance of the composites, especially in the case of CFs. After UV irradiation, the composites maintained low both CoF and WR levels. This was attributed to continuous TF formation on the counterpart. It should be noted that tribological testing in the 'start-stop' mode resulted in rising WR values *(PI; B-o-D; RT; vacuum of 10^{-4} Pa; counterpart is the GCrl5 steel ball with a diameter of 3.175 mm; R_a = n/d; V = 0.126 m/s; RR = 6 mm; P = 1 N).*

Loading with thermally conducting fillers increases the thermal conductivity and the mechanical strength of polymer composites. Debashis Puhan et al. reviewed the effect of SCFs on the TF nature and the tribological performance of the '50% PEEK + 50% PBI' composite upon friction on the steel counterpart at temperatures up to 300 °C [35]. The TF contained materials mostly related to SCFs. As a result, the CoF level reduced compared to those for neat PEEK and PBP, especially near the (TgPEEK) glass transition temperature of PEEK, when the TFs were relatively thick. At 300 °C, the 'PBP + SCF' TF became thin, possibly due to abrasion by SCFs dislodged from the matrix. Below the T_g PEEK level, the '50% PEEK + 50% PBI' composite was characterized by greater WR values than that for neat PEEK, while thick TFs formed above this temperature and wear resistance of the composite was enhanced *(PEEK-PBI; B-o-D; counterpart is the AISI 52100 steel ball with a diameter of 6 mm; R_a = n/d; DSF; P = 10 N; V = 1 and 2 m/s; T = 25, 100, 145, 200 and 300 °C; L = 3.6 km).*

In [36] Jacobs, O., et al. analyzed the effect of the counterpart material (the 100Cr6 and X5CrNi18-10 steels, alumina, and a bronze) on WR levels of PEEK-based composites loaded with CFs, GF, PTFE, and Gr at low P·V values under DSF and in an aqueous medium. At the DSF conditions, the lowest WR level was typical for stainless steel, while the best results were observed for alumina in the aqueous environment. The 'GF + PTFE' composite showed the greatest wear resistance. CFs are preferred for friction in water as they react very susceptibly with this environment. As a rule, friction in the aquatic medium contributes to increased WR values. It has been shown that the filler material can change the WR levels by several orders of magnitude at the minimum achieved level of ~10^{-8} mm^3/Nm. Correctly choosing the counterpart materials could more effectively improve wear resistance of the composites than thorough designing their compositions *(B-o-P; unidirectional sliding; R_z(100Cr6) = 0.15 µm; R_z(X5CrNi18-10) = 0.31 µm; $R_z(Al_2O_3)$ = 0.46 µm; R_z(bronze) = 0.33 µm; P = 30.0 N; P = 21.2 N; RF = 1 Hz; V = 28.2 mm/s; L = 6 km; CP = 3–27 MPa; P·V < 0.76 MPa m/s).*

Greco, A.C., et al. tested both neat PEEK and composites reinforced with short randomly oriented fibers (SROF) as well as long woven fibers (LWF) at high sliding speeds [37]. The presence (and morphology) of such fibers significantly affected the wear mechanisms under these test conditions. CoF levels decreased with increasing the load for all tested materials. The 'PEEK + LWF' composite had the lowest CoF level (50% fewer than that after loading with SROF). The same was relevant to the 'PEEK + LWF' one, whose WR value was an order of magnitude lower than that of the 'PEEK + SROF' sample. In the case of high loads, the WR level of the 'PEE + LWF' composite increased due to fracture of fibers, the abrasive wear of the counterpart surface, and TF removal *(PEEK; B-o-D; counterpart is the 440c steel ball with a diameter of 4.76 mm; ball-on-disc unidirectional sliding; R_a = n/d; P = 0.73, 2.50, 5.00 and 10.00 N; MHS = 50–600 MPa).*

When designing PI-based composites for high-temperature applications, 3-APTES and its modification with lanthanum (La) salt can be used for improving the interface properties. As an example, Yu, L., et al. investigated 'PI + poly-p-phenylenebenzobisoxazole (PBO)' samples [38]. They reported that the PBO fiber surface modification with La salt was the most efficient. CoF levels decreased for all studied composites with rising load-speed parameters at both T = 130 and 260 °C, while WR values increased in this case. In contrast to T = 130 °C, wear resistance of the unmodified composite was highly dependent on both load and speed parameters at T = 260 °C. For comparison, the modified one was less affected. Under the same tribological test parameters, the 'PI + PBO-La' composite showed the lowest specific WR and CoF levels *(PI; B-o-D; counterpart is a metal ball of 89 HRA; R_a = 0.1 μm; T = 130 and 260 °C; t = 60 min; P = 3–12 N; V = 0.25–1.00 m/s)*

Li, E.Z., et al. reported the effect of applied load and sliding duration on both CoF and WR levels of the 'PEEK + 30 wt.% GF' composite [39]. It was shown that these characteristics gradually increased and remained stable with both rising tribological test parameters. The composite possessed a markedly higher wear resistance compared to that for neat PEEK. GF were extruded from the composite rather than pulverized into it. The thermal decomposition temperature increased by 75 °C for the composite compared to that for neat PEEK. *(PEEK; B-o-D; R_a = n/d; RT; P = 100–400 N; t = 30 and 120 min).*

2.3. Solid-Lubricant Fillers

After loading with SLs, TF formation is determined by a mechanism providing an increase in the polymer wear resistance (primarily due to a decrease in CoF values). Duan, C., et al. developed an effective approach for improving the high-temperature wear resistance of thermoset PI (TPI) by loading it with g-C_3N_4 (0.5–5.0 wt.%) [40]. In a range of room temperature up to 350 °C, wear resistance of these composites improved greatly and reached 7.29×10^{-7} mm^3/Nm (T = 350 °C at the g-C_3N_4 content of 5 wt.%). The observed effect was achieved due to TF formation, containing g-C_3N_4 with both high elastic modulus and hardness levels. This enabled the composites to effectively redistribute loads on TPI and prevent resin from abrading at the contact surfaces *(PI; B-o-P; R_a(TPI) = 0.093 μm; counterpart is the GCr15 steel ring with a diameter of 3 mm; P = 5 N; V = 0.1 m/s; L = 1 km; t = 166 min; RT, 100, 200, 250, 300 and 350 °C).*

The authors of this review initially did not plan to analyze PTFE-based composites, but one such paper is of particular interest. In [41] Zhao, Y., et al. studied the effect of loading PTFE with silicon dioxide (SiO_2-PI) in amounts of 0–15 wt.% and porous PI (0–15 wt.%) on the tribological properties of the composites. Compared to loading with neat PI, the addition of SiO_2-PI and porous PI resulted in loose structures of the PTFE matrices and uneven worn composite surfaces. This promoted the formation of smooth and uniform TFs. In contrast to loading PTFE with SiO_2-PI, the addition of SiO_2 nanoparticles into the 'PTFE + PI' compounds induced the formation of rough and uniform TFs, which were detrimental to the tribological performance of the 'PTFE + PI + SiO_2' composites *(PI, B-o-F, R_a = n/d; P = 200 N; stroke length = 15 mm; frequency = 2 Hz; t = 120 min; counterpart is the GCr15 steel ball with a diameter of 9.5 mm).*

Concerning hybrid HPP-based composites, their loading with SLs and reinforcing fibers is a typical solution for improving functional properties. Song, J. investigated insulated PI-based ones filled with SGF, PTFE, SiO_2 and PPL [42]. When replacing CFs and Gr with GF and PTFE, both CoF and WR parameters were reduced. The achieved high tribological characteristics were interpreted as a synergistic effect of the simultaneous loading of the PI matrix with GF, PTFE, SiO_2, and PPL *(PI; B-o-D; counterpart is the Si3N4 ball with a diameter of 4 mm; R_a = n/d; V = 0.063 m/s; P = 3 N; t = 6 h).*

In addition to the production of bulk polymer composites, the formation of coatings is a perspective. Demian, C., et al. developed thermoset PI-based composite coatings on aluminum substrates [43]. PTFE and SiC (up to 5 wt.%) fillers were added into neat PI. It was shown that loading with PTFE significantly reduced CoF levels of the 'PI + PTFE + SiC' composite coatings, as PTFE particles contributed greatly to the reduction in the total surface energy. The 'PI + 20% PTFE + 5% SiC' composite coating was characterized by a low CoF value with a slightly decreased WR level as well as satisfactory hardness compared to those for other 'PI + PTFE + SiC' samples. *(PI; B-o-D; counterpart is the 100C6 steel ball with a diameter of 6 mm; R_a = 0.02 µm; V = 0.4–0.8 m/s; P = 5 N)* Zhang, G., et al. studied two PEEK-based coatings deposited on aluminum substrates by flame spraying and printing [44]. After annealing at 260 °C for 30 min, an initially amorphous coating obtained a semicrystalline structure, possessing both lower CoF and WR levels. The addition of SiC microparticles and Gr into the PEEK-based coatings significantly improved their wear resistance *(PEEK; B-o-D; counterpart is the 100Cr6 steel ball with the diameter of 6 mm; R_a = 0.02 µm; P = 5 N; V = 0.2 m/s; L = 2 km).*

Lal, B., et al. analyzed a series of PEEK-based composites loaded with PTFE particles (0–20 wt.%) [45]. The addition of the latter enabled enhanced ultimate load values, eliminated the stick-slip tendency, and greatly decreased both CoF and specific WR parameters. The lowest CoF value was recorded at 15% PTFE. At T = 100 °C, the CoF and WR levels increased slightly for all studied composites. On the other hand, the composites showed lower wear resistance than neat PEEK in the abrasion tribilogical mode *(PEEK, B-o-P; counterpart is the 100Cr6 steel ball with a diameter of 10 mm; R_a = n/d; frequency = 50 Hz; RT; L = 360 m; T = 100 °C; P = 50 N).*

2.4. Nanofillers

As noted above, the role of nanoparticles in HPP-based composites for tribological applications narrows to (1) reinforcing the polymer matrix; (2) (solid) lubricating (with correct compositions); (3) stimulating TF fixation on counterparts. The most 'popular' types of nanofillers were also listed. Results of a number of papers devoted to the point composite-counterpart contacts are summarized below.

Zhao, Y., et al. fabricated 'PI + nano-SiO_2' (0–25 wt.%) composites via in situ polymerization [46]. First, CoF levels of the composites decreased by 6.8% with an increase in the nano-SiO_2 content from 0 to 5 wt.%. Then, they enhanced CoF levels by 11% with raising the content up to 25 wt.%. At the nano-SiO_2 contents of 5–10 wt.%, WR values of the composites were greater than that for neat PI. Formed TFs delaminated easily, and nano-SiO_2 particles tended to be accumulated on the friction surfaces. These factors reduced wear resistance of the composites (*PI; B-o-D; R_a = n/d; RT; t = 1.5 h; V = 0.04 and 0.08 m/s; P = 5 and 10 N; counterpart is the GCr15 ball with a diameter of 3 mm*). Zhou S., et al. investigated PI-based composite coatings composed of CNTs and fluorinated graphene (FG), in which both hybrid and blend phases were mixed via solution doping [47]. A significant increase in the mechanical properties was accompanied by a decrease in WR levels by 61%. For the 'PI + CNT + FG' composite coating, the CNT strengthening effect and the FG lubrication characteristics were fully manifested in the blend phase *(PI; B-o-D; R_a = n/d; SF = 2 Hz; DSF; t = 30 min; P = 5 N; counterpart is the GCr15 steel ball with the diameter of 3 mm).*

In [48] Chen, B., et al. prepared multiscale 'CF + CNT' PI-based composites using a chemical method. The composites possessed many functional groups and increased roughness. CoF and WR values of the 'PI + CF + CNT' composites were 0.213 and 1.79 × 10^{-6} mm^3/Nm, i.e., decreased by 22% and 72%, respectively, compared to those for neat PI. Also, both CoF and WR levels decreased by raising the load-speed product. Thus, CNTs stretched into the PI matrix on the hybrid 'CF + CNT' surface, which had a reinforcing effect even at high load-speed parameters *(B-o-F; RS; counterpart is the GCr15 ball; R_a = n/d; DSF; t = 30 min; P = 1.5–4.5 N; LRV; V = 0.05, 0.083 and 0.116 m/s).*

Nanofillers are made in complex shapes to improve their adhesion. Yuan, H., et al. loaded PI with MoS_2 nanoflowers (0.5–1.5 wt.%) through grafting them onto the surfaces of hollow CNFs (HCNFs) [49]. The 'PI + MoS_2 + HCNF' composite coatings showed high wear resistance under WL conditions (with a filler content of 0.5 wt.%, the WR reduction was 72.5%) and in liquid paraffin oil (with a filler content of 1.5 wt.%, the WR value decreased by 56.0%) *(PI; B-o-P; the counterpart is the GCr15 steel ball with a diameter of 6 mm; R_a=; RT; RH = 25–30%; HCP = 112 MPa; P = 20 N; V = 1.2 cm/s (20 Hz); t = 30 min).* Graphitic carbon nitride (g-C_3N_4) is being extensively investigated by many researchers as a nanofiller for improving the tribological properties of PI-based composites. For example, Zhu, L., et al. showed [50] that its contents from 0.5 up to 2.0 wt.% had a decisive influence on the tribological properties of the 'PI + g-C_3N_4' composites. CoF kinetics gradually decreased with raising the g-C_3N_4 filler concentration but increased above 10 wt.%. At its low contents, the wear type was adhesive, while it changed to abrasive with excessive g-C_3N_4 levels *(PI; B-o-D; R_a = n/d; DSF; reciprocating testing; P = 2, 4 and 50 N; counterpart is the GCr15 ball with the diameter of 6 mm; t = 10 min; V = 0.42 m/s; RT; RH = 40%).*

Chen, B., et al. designed a novel hybrid PI-based composite with micro-CFs and hexagonal MoS_2 nanosheets (0.5–20.0 wt.%) via a one-step hydrothermal method [51]. The hybrid simultaneously exerted both lubricating and strengthening effects on the PI matrix. This contributed to transferring stresses from the matrix to CFs during friction and wear. The 'PI + CF + MoS_2' composite showed advanced tribological properties. CoF and WR values were equal to only 0.24 and 2.01×10^{-6} mm^3/Nm, respectively, which were lower than those for neat PI, as well as for both 'PI + CF' and 'PI + MoS_2' composites. Additionally, self-lubricating MoS_2 nanosheets gradually exposed on the worn surfaces, making it easier to slide *(PI, B-o-F; R_a = n/d; P = 3 N; V = 0.083 m/s; t = 30 min).*

Min, C., et al. fabricated PI-based nanocomposites using different contents of amine-functionalized graphene nanosheets (AGNS) via in situ polymerization [52]. In contrast to neat PI and 'PI + GNS' composites, the 'PI + 0.5 wt.% AGNS' sample was characterized by both reduced CoF and specific WR (by 41.9% and 72.6%, respectively. Under DSF conditions, this effect was provided by strong interfacial adhesion and good compatibility between AGNS and PI (**Figure 8**). In addition, the 'PI + AGNS' nanocomposite showed excellent wear resistance in seawater at CoF = 0.16 and WR = $1.68 \cdot 10^{-4}$ mm^3/Nm *(PI, B-o-D; R_a = n/d; DSF, SWL; V = 300 r/min; t = 30 min; P = 5 N; the counterpart is the GCr15 steel ball with a diameter of 4 mm).*

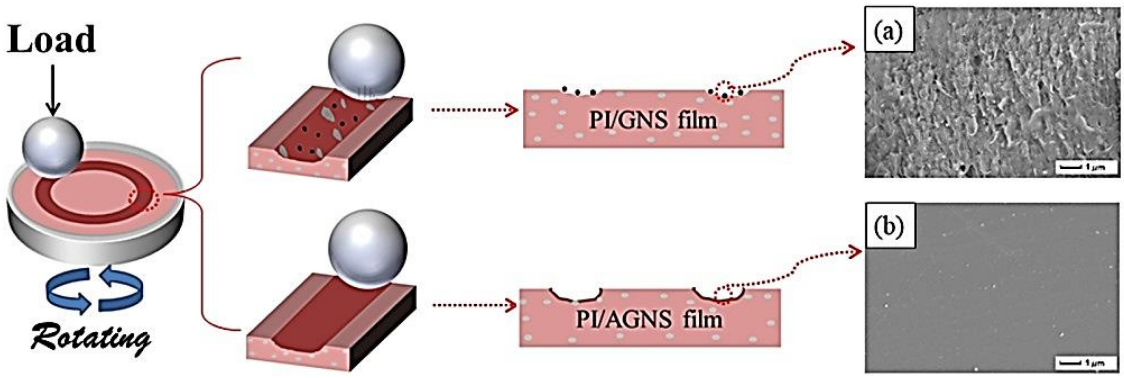

Figure 8. A model of the friction mechanism for the 'PI + GNS' and 'PI + AGNS' films. The inset is the SEM images of worn surface of (**a**) PI/GNS-1wt.% nanocomposite and (**b**) PI/AGNS-1wt.% nanocomposite. Figure is reproduced with permission from reference [52].

Zhou, S., et al. investigated 'PI + FG' nanocomposite films (FG is fluorinated graphene in amounts of 0.5–2.0 wt.%) under different friction conditions [53]. CoF levels of the nanocomposites decreased slightly compared to that for neat PI. During the DSF tribological test, a WR value reduced by 51.2% for the composite with the optimum filler content of 0.5%. However, the WR levels decreased significantly for all samples due to the softening effect of water on the 'PI + FG' mixture, indicating that they were unsuitable for operation in aqueous environments. The presence of products of tribochemical reactions on the wear track surfaces provided an antiwear effect and reduced the CoF values (**Figure 9**). The FG layer covered the steel counterpart surface and formed a dense TF. Also, it reduced the CoF values and improved wear resistance *(PI; B-o-D; the counterpart is the GCr15 steel ball with a diameter of 3 mm; R_a = n/d; frequency = 5 Hz; P = 10 N; t = 30 min; DSF, SLF).* Min, C., et al. designed the 'PI + 0.5 wt.% FGO' nanocomposite [54]. Due to covalent bonds, the great FGO to PI interfacial adhesion increased their mechanical

strength and wear resistance. At 0.5 wt.% FGO nanosheets, both CoF and WR parameters were reduced by 33.1% and 80.8%, respectively, compared to neat PI under the DSF conditions. In SWL, a CoF level was equal to 0.22, while the WR value of $0.45 \cdot 10^{-4}$ mm^3/Nm was registered *(PI, B-o-D; R_a = n/d; DSF and SWL; P = 5 N; V = 300 r/min; t = 30 min).*

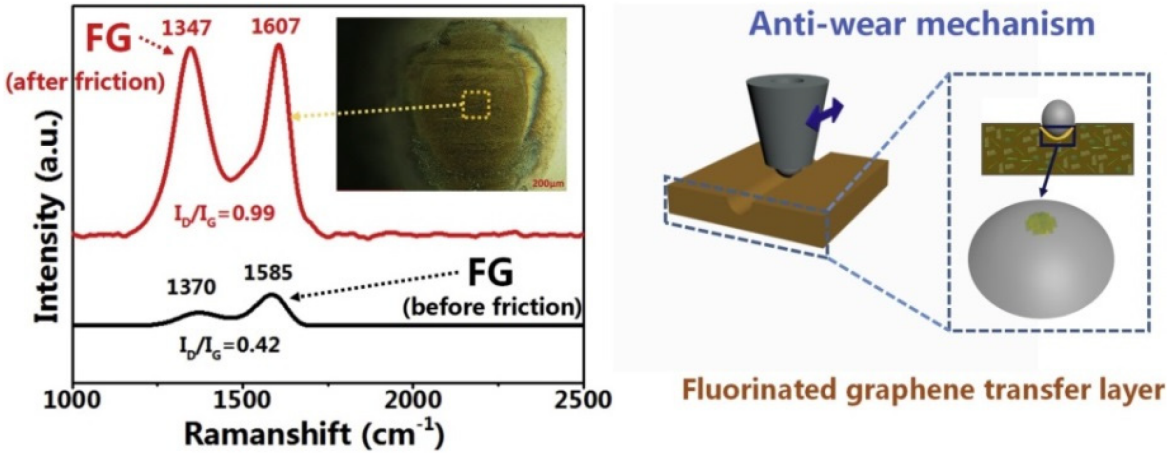

Figure 9. A schematic presentation of the tribological mechanism for the 'PI + FG' nanocomposites. Figure is reproduced with permission from reference [53].

In [55] Zhao, Z., et al. used CeO_2 nanoparticles (about 80–110 nm, 0–9 wt.%, prepared via in situ synthesis) for strengthening 'PAI + PTFE' coatings. At a concentration of CeO_2 nanoparticles of 5 wt.%, the worn coating surface was the least damaged. During friction, substance transfer was observed, accompanied by tribochemical reactions. Due to TF formation, it was possible to exclude direct contact between the components of the mating materials (**Figure 10**), which improved their wear resistance. It was concluded that the 'PAI + PTFE' coatings are more suitable for high sliding speeds at low loads *(PAI; B-o-F; R_a = n/d; LRF; Dist = 5 mm; P = 5 N; V = 10 cm/s; L = 400 m; RT; AH = 35–55%).*

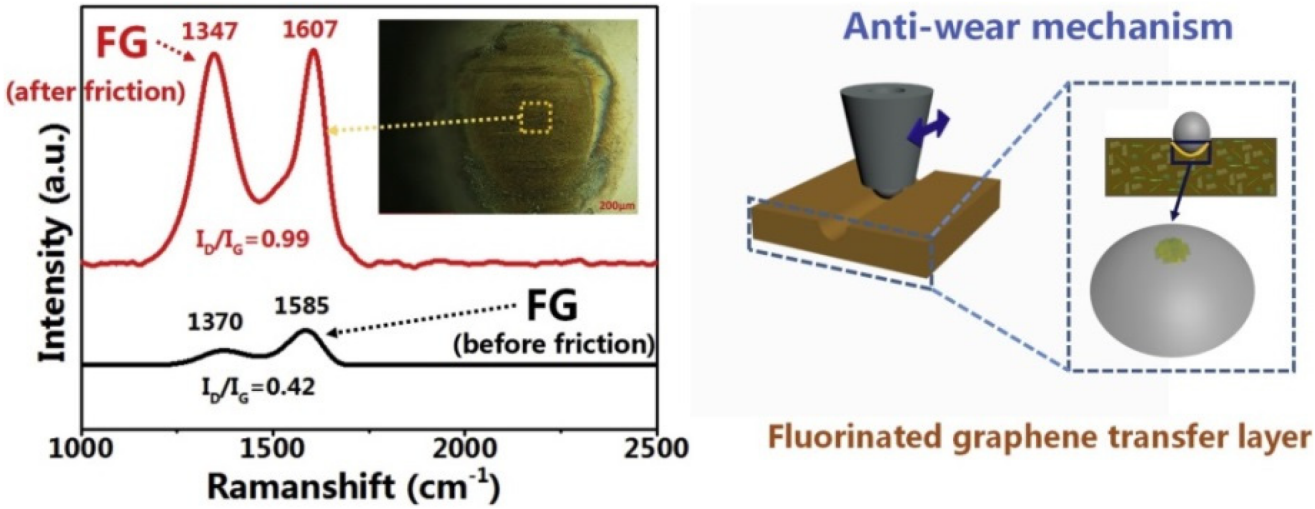

Figure 10. (**a**) Results of XRD analysis of the worn 'PAI + PTFE' coating surface and (**b**) a scheme of the tribochemical reactions. Figure is reproduced with permission from reference [55].

Puértolas, J. A., et al. used the lubricant capability of graphene nanoplatelets (GNPs) to improve PEEK tribological properties [56]. Nanocomposites were fabricated by solvent-free melt-blending and injection molding at the filler contents of 1–10 wt.%. The CoF reduction was about 83% for the 'PEEK + 10% GNP' composite. This effect was associated with an increase in its hardness. At high GNP contents, the wear mechanism was fatigue, while the abrasive one dominated at the lowest concentrations. At the filling degrees of 3–5 wt.%, it was possible to reduce both CoF and WR at constant elastic modulus and strength levels *(PEEK; B-o-D; R_a(PEEK) = 1 μm; counterpart is the alumina ball with a diameter of 6 mm; R_a = 0.050 ± 0.002 μm; WL; T = 37 °C; P = 5 N; HCP = 37 MPa; V = 0.05 m/s; L = 0.18, 2.16 and 4.52 km).* Due to the widespread use of PEEK in the field of artificial joint materials, Ting Wu et al. in situ integrated nano-ZnO particles (2.5–7.5 wt.%) in the PEEK powder surfaces by a one-step hydrothermal method [57]. As a result, their compressive strength reached 319 MPa, while the lowest WR level was 0.48 × 10^{-6} mm^3/Nm for the 'PEEK + 5% nano-ZnO' composite, which was 68% lower than that for neat PEEK, according to **Figure 11** *(PEEK; P-o-D; R_a = n/d; RLS; counterpart is the CoCrMo pin with a diameter of 10 mm; Dist = 10 mm; P = 30 N; V = 5 mm/s; t = 120 min; RT; 25% CSL).*

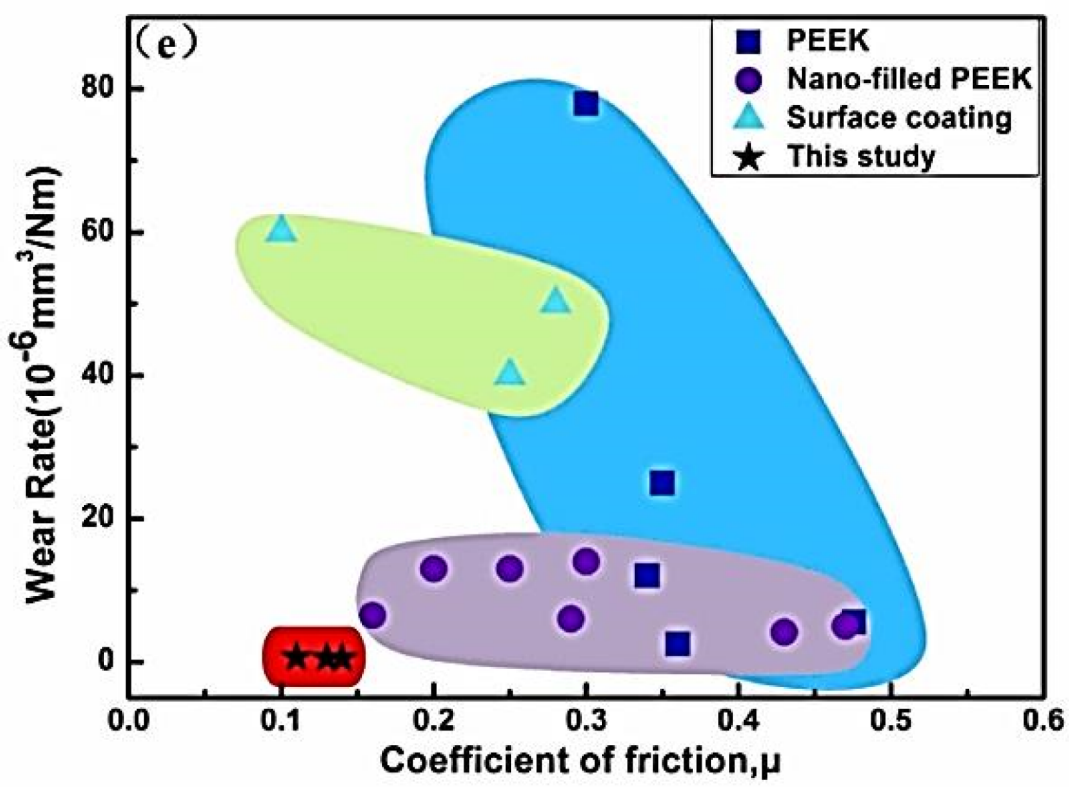

Figure 11. The WR vs. CoF diagram by Ashby (Zhang, 2010; Panin et al., 2021; Yan et al., 2020; Wang et al., 2017; Tharajak et al., 2015, 2017). Figure is reproduced with permission from reference [57].

As a summary of this section, it is appropriate to cite the paper [58] by Guo, L., et al., that reviews papers on tribological test results of PEEK-based composites using the pin-on-disk scheme published in the last 20 years and

provides new experimental data. In their research, PEEK was reinforced with CFs and loaded with Bi_2O_3 and SiO_2 nanoparticles, as well as with conventional SLs (Gr and PTFE). SL particles improved wear resistance at low sliding speeds, especially with negligible loads. Chelation reactions between PTFE and the steel counterpart, as well as transfer of graphitic materials deriving Gr and CF debris were the main mechanisms driving TF growth. When sliding at a P = 1 MPa and speeds from 0.05 up to 0.20 m/s, additional loading with Bi_2O_3 nanoparticles significantly reduced WR levels of the CF-reinforced PEEK-based composite. At higher pressures or lower speeds, the effect of Bi_2O_3 nanoparticles was negligible. At low loads and relatively high speeds, releasing Bi_2O_3 nanoparticles on the friction surface improved TF load-bearing capability. The positive role of SiO_2 nanoparticles was manifested at P = 30 MPa and V = 0.1 m/s. In the case of sliding at P = 30 MPa and V = 0.01 m/s, a great load and a relatively high speed contributed to the formation of strong TF reinforced with SiO_2. The antiwear role of the SLs was the most pronounced at both low loads and speeds *(PEEK; P-o-D; counterparts are polymer pins and the GCr15 steel disk; R_a = 0.25 μm; DSF; RT; radius = 16.5 mm; V = 0.01–0.20 m/s; P = 1–30 MPa; t = 5 h).*

References

1. Briscoe, B.J.; Sinha, S.K. Chapter 1—Tribological applications of polymers and their composites–past, present and future prospects. In Tribology of Polymeric Nanocomposites. Friction and Wear of Bulk Materials and Coatings, 2nd ed.; Friedrich, K., Schlarb, A., Eds.; Butterworth-Heinemann: Oxford, UK, 2013; pp. 1–22.
2. Bahadur, S.; Schwartz, C. Chapter 2—The effect of nanoparticle fillers on transfer film formation and the tribological behavior of polymers. In Tribology of Polymeric Nanocomposites. Friction and Wear of Bulk Materials and Coatings, 2nd ed.; Friedrich, K., Schlarb, A., Eds.; Butterworth-Heinemann: Oxford, UK, 2013; pp. 23–48.
3. Chang, L.; Zhang, Z.; Ye, L.; Friedrich, K. Chapter 3—Synergistic effects of nanoparticles and traditional tribofillers on sliding wear of polymeric hybrid composites. In Tribology of Polymeric Nanocomposites. Friction and Wear of Bulk Materials and Coatings, 2nd ed.; Friedrich, K., Schlarb, A., Eds.; Butterworth-Heinemann: Oxford, UK, 2013; pp. 49–89.
4. Padhan, M.; Marathe, U.; Bijwe, J. Tribology of Poly(etherketone) composites based on nano-particles of solid lubricants. Compos. Part B Eng. 2020, 201, 108323.
5. Wang, Q.; Pei, X. Chapter 4—The influence of nanoparticle fillers on the friction and wear behavior of polymer matrices. In Tribology of Polymeric Nanocomposites. Friction and Wear of Bulk Materials and Coatings, 2nd ed.; Friedrich, K., Schlarb, A., Eds.; Butterworth-Heinemann: Oxford, UK, 2013; pp. 91–118.
6. Ashby, M.F. Materials Selection in Mechanical Design, 4th ed.; Butterworth-Heinemann: Oxford, UK, 2011; p. 646.

7. Ren, Y.; Zhang, L.; Xie, G.; Li, Z.; Chen, H.; Gong, H.; Xu, W.; Guo, D.; Luo, J. A review on tribology of polymer composite coatings. Friction 2021, 9, 429–470.
8. Kurdi, A.; Chang, L. Recent Advances in High Performance Polymers—Tribological Aspects. Lubricants 2019, 7, 2.
9. De Leon, A.C.C.; da Silva, Í.G.M.; Pangilinan, K.D.; Chen, Q.; Caldona, E.B.; Advincula, R.C. High performance polymers for oil and gas applications. React. Funct. Polym. 2021, 162, 104878.
10. Theivendran, K.; Arshad, F.; Hanif, U.; Reito, A.; Griffin, X.; Foot, C.J. Carbon fibre reinforced PEEK versus traditional metallic implants for orthopaedic trauma surgery: A systematic review. J. Clin. Orthop. Trauma 2021, 23, 101674.
11. Oladapo, B.I.; Zahedi, S.A.; Ismail, S.O.; Omigbodun, F.T. 3D printing of PEEK and its composite to increase biointerfaces as a biomedical material—A review. Colloids Surf. B 2021, 203, 111726.
12. Verma, S.; Sharma, N.; Kango, S.; Sharma, S. Developments of PEEK (Polyetheretherketone) as a biomedical material: A focused review. Eur. Polym. J. 2021, 147, 110295.
13. Alexakou, E.; Damanaki, M.; Zoidis, P.; Bakiri, E.; Mouzis, N.; Smidt, G.; Kourtis, S. PEEK High Performance Polymers: A Review of Properties and Clinical Applications in Prosthodontics and Restorative Dentistry. Eur. J. Prosthodont. Restor. Dent. 2019, 27, 113–121.
14. Oladapo, B.I.; Zahedi, S.A.; Omigbodun, F.T. A systematic review of polymer composite in biomedical engineering. Eur. Polym. J. 2021, 154, 110534.
15. Ma, H.; Suonan, A.; Zhou, J.; Yuan, Q.; Liu, L.; Zhao, X.; Lou, X.; Yang, C.; Li, D.; Zhang, Y. PEEK (Polyether-ether-ketone) and its composite materials in orthopedic implantation. Arab. J. Chem. 2021, 14, 102977.
16. Singh, S.; Prakash, C.; Wang, H.; Yu, X.; Ramakrishna, S. Plasma treatment of polyether-ether-ketone: A means of obtaining desirable biomedical characteristics. Eur. Polym. J. 2019, 118, 561–577.
17. Veazey, D.; Hsu, T.; Gomez, E.D. Next generation high-performance carbon fiber thermoplastic composites based on polyaryletherketones. J. Appl. Polym. Sci. 2016, 134, 44441.
18. Liaw, D.J.; Wang, K.L.; Huang, Y.C.; Lee, K.R.; Lai, J.Y.; Ha, C.S. Advanced polyimide materials: Syntheses, physical properties and applications. Prog. Polym. Sci. 2012, 37, 907–974.
19. Ogbonna, V.E.; Popoola, P.I.; Popoola, O.M.; Adeosun, S.O. A review on recent advances on improving polyimide matrix nanocomposites for mechanical, thermal, and tribological applications: Challenges and recommendations for future improvement. J. Thermoplast. Compos. Mater. 2021, 089270572110079.
20. Ogbonna, V.E.; Popoola, A.P.I.; Popoola, O.M.; Adeosun, S.O. A review on polyimide reinforced nanocomposites for mechanical, thermal, and electrical insulation application: Challenges and

recommendations for future improvement. Polym. Bull. 2020, 79, 663–695.

21. Constantin, C.P.; Aflori, M.; Damian, R.F.; Rusu, R.D. Biocompatibility of Polyimides: A Mini-Review. Materials 2019, 12, 3166.
22. Puhan, D.; Wong, J. Properties of Polyetheretherketone (PEEK) transferred materials in a PEEK-steel contact. Tribol. Int. 2019, 135, 189–199.
23. Wang, M. The tribological performance of engineered micro-surface topography by picosecond laser on PEEK. Ind. Lubr. Tribol. 2019, 72, 172–179.
24. Cho, M. Friction and wear of a hybrid surface texturing of polyphenylene sulfide-filled micropores. Wear 2016, 346–347, 158–167.
25. Duan, C.; Yang, Z.; Zhang, D.; Tao, L.; Wang, Q.; Wang, T. Effect of isomerism on mechanical and tribological properties of thermoplastic polyimide films. Tribol. Int. 2018, 121, 373–380.
26. Fareed, M.I. Effect of operating conditions on the tribological performance of polyether ether ketone (PEEK). Adv. Polym. Technol. 2018, 37, 1537–1543.
27. Tatsumi, G.; Ratoi, M.; Shitara, Y.; Sakamoto, K.; Mellor, B.G. Effect of organic friction modifiers on lubrication of PEEK-steel contact. Tribol. Int. 2020, 151, 106513.
28. Laux, K.A.; Jean-Fulcrand, A.; Sue, H.J.; Bremner, T.; Wong, J.S.S. The influence of surface properties on sliding contact temperature and friction for polyetheretherketone (PEEK). Polymer 2016, 103, 397–404.
29. Yahiaoui, M.; Chabert, F.; Paris, J.Y.; Nassiet, V.; Denape, J. Friction, acoustic emission, and wear mechanisms of a PEKK polymer. Tribol. Int. 2019, 132, 154–164.
30. Jean-Fulcrand, A.; Masen, M.A.; Bremner, T.; Wong, J.S.S. Effect of temperature on tribological performance of polyetheretherketone-polybenzimidazole blend. Tribol. Int. 2019, 129, 5–15.
31. Zhang, G.; Zhang, C.; Nardin, P.; Li, W.Y.; Liao, H.; Coddet, C. Effects of sliding velocity and applied load on the tribological mechanism of amorphous poly-ether–ether–ketone (PEEK). Tribol. Int. 2008, 41, 79–86.
32. Yamaguchi, T.; Hokkirigawa, K. Friction and Wear Properties of PEEK Resin Filled with RB Ceramics Particles under Water Lubricated Condition. Tribol. Online 2016, 11, 653–660.
33. Dong, F.; Hou, G.; Cao, F.; Yan, F.; Liu, L.; Wang, J. The lubricity and reinforcement of carbon fibers in polyimide at high temperatures. Tribol. Int. 2016, 101, 291–300.
34. Lv, M.; Zheng, F.; Wang, Q.; Wang, T.; Liang, Y. Friction and wear behaviors of carbon and aramid fibers reinforced polyimide composites in simulated space environment. Tribol. Int. 2015, 92, 246–254.

35. Puhan, D.; Jiang, S.; Wong, J.S.S. Effect of carbon fiber inclusions on polymeric transfer film formation on steel. Compos. Sci. Technol. 2022, 217, 109084.
36. Jacobs, O.; Jaskulka, R.; Yan, C.; Wu, W. On the effect of counterface material and aqueous environment on the sliding wear of various PEEK compounds. Tribol. Lett. 2005, 18, 359–372.
37. Greco, A.C.; Erck, R.; Ajayi, O.; Fenske, G. Effect of reinforcement morphology on high-speed sliding friction and wear of PEEK polymers. Wear 2011, 271, 2222–2229.
38. Yu, L.; Zhang, Y.; Tang, J.; Gao, J. Friction and Wear Behavior of Polyimide Composites Reinforced by Surface-Modified Poly-p-Phenylenebenzobisoxazole (PBO) Fibers in High Ambient Temperatures. Polymers 2019, 11, 1805.
39. Li, E.Z.; Guo, W.L.; Wang, H.D.; Xu, B.S.; Liu, X.T. Research on Tribological Behavior of PEEK and Glass Fiber Reinforced PEEK Composite. Phys. Procedia 2013, 50, 453–460.
40. Duan, C.; Yuan, D.; Yang, Z.; Li, S.; Tao, L.; Wang, Q.; Wang, T. High wear-resistant performance of thermosetting polyimide reinforced by graphitic carbon nitride (g-C3N4) under high temperature. Compos. Part A Appl. Sci. Manuf. 2018, 113, 200–208.
41. Zhao, Y.; Qi, X.; Ma, J.; Dong, Y.; Yang, Y. Effects of polyimide/silica and polyimide/pores fillers on the morphology, thermal, mechanical, and tribological properties of polytetrafluoroethylene composites. Polym. Compos. 2019, 41, 1435–1446.
42. Song, J.; Yu, Y.; Zhao, G.; Qiu, J.; Ding, Q. Comparative study of tribological properties of insulated and conductive polyimide composites. Friction 2020, 8, 507–516.
43. Demian, C.; Liao, H.; Lachat, R.; Costil, S. Investigation of surface properties and mechanical and tribological behaviors of polyimide based composite coatings. Surf. Coat. Technol. 2013, 235, 603–610.
44. Zhang, G.; Li, W.Y.; Cherigui, M.; Zhang, C.; Liao, H.; Bordes, J.M.; Coddet, C. Structures and tribological performances of PEEK (poly-ether-ether-ketone)-based coatings designed for tribological application. Prog. Org. Coat. 2007, 60, 39–44.
45. Lal, B.; Alam, S.; Mathur, G.N. Tribo-investigation on PTFE lubricated PEEK in harsh operating conditions. Tribol. Lett. 2007, 25, 71–77.
46. Zhao, Y.; Qi, X.; Dong, Y.; Ma, J.; Zhang, Q.; Song, L.; Yang, Y.; Yang, Q. Mechanical, thermal and tribological properties of polyimide/nano-SiO2 composites synthesized using an in-situ polymerization. Tribol. Int. 2016, 103, 599–608.
47. Zhou, S.; Li, W.; Zhao, W.; Li, Q.; Liu, C.; Fang, Z.; Gao, X. Tribological behaviors of polyimide composite coatings containing carbon nanotubes and fluorinated graphene with hybrid phase or blend phase. Prog. Org. Coat. 2020, 147, 105800.

48. Chen, B.; Li, X.; Li, X.; Jia, Y.; Yang, J.; Yang, G.; Li, C. Friction and Wear Properties of Polyimide-Based Composites with a Multiscale Carbon Fiber-Carbon Nanotube Hybrid. Tribol. Lett. 2017, 65, 111.
49. Yuan, H.; Yang, S.; Liu, X.; Wang, Z.; Ma, L.; Hou, K.; Yang, Z.; Wang, J. Polyimide-based lubricating coatings synergistically enhanced by MoS2@HCNF hybrid. Compos. Part A Appl. Sci. Manuf. 2017, 102, 9–17.
50. Zhu, L.; You, L.; Shi, Z.; Song, H.; Li, S. An investigation on the graphitic carbon nitride reinforced polyimide composite and evaluation of its tribological properties. J. Appl. Polym. Sci. 2017, 134, 45403.
51. Chen, B.; Li, X.; Jia, Y.; Li, X.; Yang, J.; Yan, F.; Li, C. MoS2 nanosheets-decorated carbon fiber hybrid for improving the friction and wear properties of polyimide composite. Compos. Part A Appl. Sci. Manuf. 2018, 109, 232–238.
52. Min, C.; Liu, D.; Qian, J.; He, Z.; Jia, W.; Song, H.; Guo, L. High mechanical and tribological performance polyimide nanocomposites using amine-functionalized graphene nanosheets. Tribol. Int. 2019, 131, 1–10.
53. Zhou, S.; Li, W.; Zhao, W.; Liu, C.; Fang, Z.; Gao, X. Tribological behaviors of polyimide composite films enhanced with fluorographene. Colloids Surf. A 2019, 580, 123707.
54. Min, C.; He, Z.; Liang, H.; Liu, D.; Dong, C.; Song, H.; Huang, Y. High mechanical and tribological performance of polyimide nanocomposite reinforced by fluorinated graphene oxide. Polym. Compos. 2020, 41, 1624–1635.
55. Zhao, Z.; Ma, Y.; Wan, H.; Ye, Y.; Chen, L.; Zhou, H.; Chen, J. Preparation and tribological behaviors of polyamide-imide/polytetrafluoroethylene lubricating coatings reinforced by in-situ synthesized CeO2 nanoparticles. Polym. Test. 2021, 96, 107100.
56. Puértolas, J.A.; Castro, M.; Morris, J.A.; Ríos, R.; Ansón-Casaos, A. Tribological and mechanical properties of graphene nanoplatelet/PEEK composites. Carbon 2019, 141, 107–122.
57. Wu, T.; Zhang, X.; Chen, K.; Chen, Q.; Yu, Z.; Feng, C.; Qi, J.; Zhang, D. The antibacterial and wear-resistant nano-ZnO/PEEK composites were constructed by a simple two-step method. J. Mech. Behav. Biomed. Mater. 2022, 126, 104986.
58. Guo, L.; Pei, X.; Zhao, F.; Zhang, L.; Li, G.; Zhang, G. Tribofilm growth at sliding interfaces of PEEK composites and steel at low velocities. Tribol. Int. 2020, 151, 106456.